



Cite this: *Polym. Chem.*, 2022, **13**, 3949

## Perfluorocyclobutyl-containing transparent polyimides with low dielectric constant and low dielectric loss<sup>†</sup>

Weifeng Peng,<sup>a</sup> Huanyu Lei,<sup>a</sup> Luhao Qiu,<sup>a</sup> Feng Bao<sup>a</sup> and Mingjun Huang  <sup>a,b</sup>

Polymers with low dielectric permittivity and dielectric loss are essential for the microelectronics and wireless communication industries. The perfluorocyclobutyl (PFCB) aryl ether group has been proven to afford polymer materials with a high fluorine content and large free volume, resulting in many attractive properties, *e.g.*, good thermal and chemical stability, high hydrophobicity, transparency and low dielectric permittivity. Herein, a series of PFCB-containing polyimides were designed and synthesized. The conformational isomers of the diamine monomer could be separated, providing an opportunity to explore the effects of the isomer conformations on the polyimide properties. All these PFCB-containing polyimides present relatively loose chain packings due to their strongly distorted chain conformations. The combined loose chain packing and high fluoro content afford these PFCB-containing polyimides excellent optical transparency and dielectric properties. In particular, dielectric permittivity and dielectric loss values as low as 2.50 and 0.0035 at high frequency (10 GHz) were obtained, enabling potential applications in the microelectronics industry.

Received 28th April 2022,  
Accepted 18th June 2022

DOI: 10.1039/d2py00550f  
[rsc.li/polymers](http://rsc.li/polymers)

## Introduction

Polymers with excellent dielectric properties have drawn great attention in the field of integrated circuits (ICs), especially for ultra-large-scale integration (ULSI) circuits and high-speed IC packing, as well as for flexible printed circuit boards (FPCBs) at high frequency.<sup>1–5</sup> With the rapid development of ULSI circuits, advanced chips generally integrate billions of transistors. The average size of metal interconnects has shrunk to the order of 10 nm; however, this is accompanied with increased wire resistance and RC signal delay. These issues strongly limit the performance of devices, including increased device loss and reduced service life.<sup>6</sup> Commercial dielectric materials, *e.g.*, silicon dioxide ( $\text{SiO}_2$ ), seem unable to fully satisfy the requirements of ULSIs, creating a demand for other advanced dielectric materials.<sup>3,7</sup> Polymer dielectric materials have great advantages over their inorganic counterparts for ULSIs, including light weight, good processability, and flexible and versatile

structure modification.<sup>8–10</sup> Thus, the development of dielectric polymers with improved performance is of great significance to the electronics and communications industries.

Dielectric polymers with high thermal stability are strictly required for the production of microprocessor chips, in which metal wire bonding is involved.<sup>11</sup> Among the diverse high-performance polymer materials, polyimides are known as a “problem solver” because of their excellent integrative properties including excellent flexibility, thermal stability, solvent resistance and mechanical strength.<sup>12–15</sup> Nonetheless, the polar imide group endows the polyimide with a relatively high dielectric constant (around 3.5), which does not meet the requirements of the microelectronics industry.<sup>16</sup> From the perspective of molecular structure design, there are two main strategies to lower the dielectric constant in polyimides: one is introducing large pendant groups to decrease the packing density of the polyimide chains;<sup>5,17–19</sup> the other is increasing the amount of fluorine atoms on the polyimide backbone to reduce the polarization ability.<sup>20–22</sup> These two strategies could also be combined to further decrease the dielectric constant.<sup>21</sup>

The perfluorocyclobutyl aryl ether (PFCB) group has been proven to afford polymer materials with high fluorine content and large free volume, resulting in many attractive properties, *e.g.*, good thermal and chemical stability, high hydrophobicity, transparency and low dielectric permittivity.<sup>23–26</sup> PFCB-containing polymers have demonstrated good performance in photoelectric materials, non-wetting electro-spun surfaces,

<sup>a</sup>South China Advanced Institute for Soft Matter Science and Technology, School of Emergent Soft Matter, South China University of Technology, Guangzhou 510640, China. E-mail: huangmj25@scut.edu.cn

<sup>b</sup>Guangdong Provincial Key Laboratory of Functional and Intelligent Hybrid Materials and Devices, South China University of Technology, Guangzhou 510640, China

<sup>†</sup> Electronic supplementary information (ESI) available. See DOI: <https://doi.org/10.1039/d2py00550f>

light-emitting and hole-transporting materials, proton exchange membranes, dielectric materials in ICs and FPCBs, *etc.*<sup>23</sup> The integration of the PFCB group into polyimides was reported by Huang *et al.*<sup>27,28</sup> The PFCB-containing yellow polyimides showed improved dielectric properties and low water absorption.

In this work, a series of transparent polyimides with high PFCB content are designed and synthesized (Scheme 1a). The PFCB-containing dianhydride and diamine monomers 5,5'-(*perfluorocyclobutane-1,2-diyil*)bis(*oxy*)bis(isobenzofuran-1,3-dione) (PFODPA) and 4,4'-(*perfluorocyclobutane-1,2-diyil*)bis(*oxy*)dianiline (PFODA) were synthesized successfully. It is worth noting that the isomers of PFODA could be separated based on the minor difference in their polarities (Fig. S1†), providing an opportunity to explore the effects of the isomer conformation on the polyimide properties. 4,4'-(*Hexafluoroisopropylidene*)diphthalic anhydride (6FDA) and bis(*trifluoromethyl*)-4,4'-diaminobiphenyl (TFMB) were chosen for polymerization with PFODA and PFODPA with the aim of lowering the dielectric constant and dielectric loss. The intro-

duction of the PFCB group with its distorted conformation and high fluorine content endows the polyimides with various advantages, *e.g.*, excellent processability, hydrophobicity, high optical transparency and attractive dielectric properties. All these PFCB-containing polyimides present a low dielectric constant (<2.5) and dielectric loss (<0.01). In particular, the 6FDA-*co*-PFODPA-PFODA copolymerized film possesses an ultra-low dielectric constant value of 2.36 and dielectric loss of  $1.3 \times 10^{-3}$  at 1 kHz, and a dielectric constant of 2.5 and dielectric loss of  $3.5 \times 10^{-3}$  at 10 GHz. These PFCB-containing polyimide films may have potential applications in the electronics industry, *e.g.*, as the dielectric layer in ULSI and the substrate film in FPCB at high frequency.

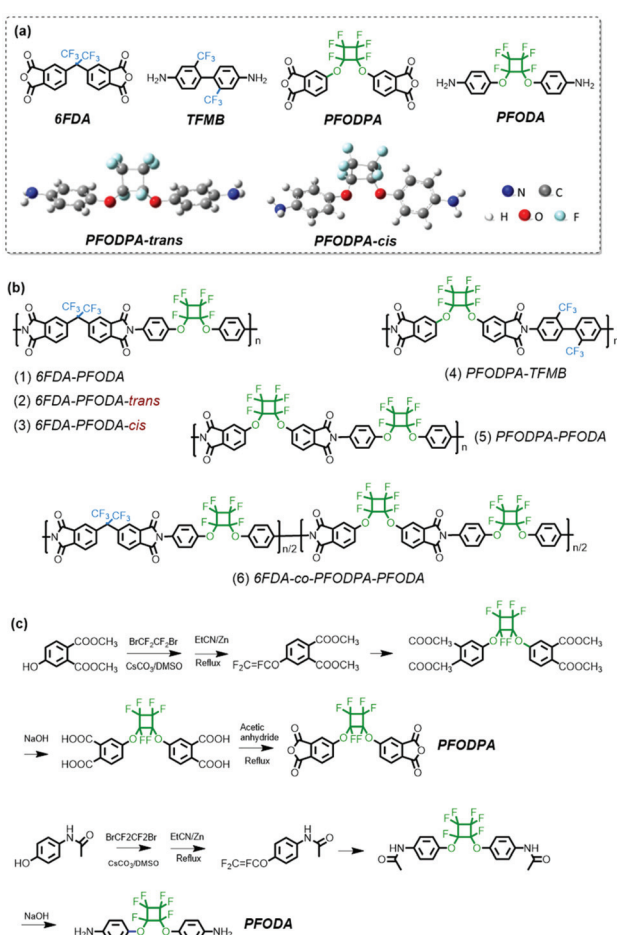
## Results and discussion

### Structural characterization of monomers (PFODPA and PFODA)

The structure of the fluorinated monomers plays a vital role in determining the properties of the materials. The availability of commercial fluorine-containing monomers is limited, especially dianhydride monomers. Here, PFCB-containing dianhydride (PFODPA) and diamine (PFODA) monomers were synthesized (Scheme 1c). As reported previously in the literature,<sup>29</sup> the *cis* and *trans* conformational isomers of perfluorocyclobutyl aryl ether were present with a distribution ratio of 1 : 1. Density functional theory (DFT) calculations were utilized to analyze the differences between the conformations, and revealed that the *cis* and *trans* conformations of both the PFODPA and PFODA monomers have almost the same minimized-energy state (Table S1†). Although numerous PFCB-containing polymers have been reported, the influence of PFCB conformational isomers on material properties has rarely been studied. Luckily, the two isomers of PFODA present a minor polarity difference ( $\Delta R_f = 0.05$ ) in silica chromatography (Fig. S1†). The optimized geometries of the PFODA isomers are shown in Scheme 1a. PFODA-*trans* possesses lower polarity and elutes first from the silica column. This polarity difference was also observed in the DFT calculations, with PFODA-*cis* showing a higher dipole moment (3.11 Debye) than PFODA-*trans* (1.24 Debye). These two isomers were separated and confirmed by  $^1\text{H}$ ,  $^{13}\text{C}$ , and  $^{19}\text{F}$  nuclear magnetic resonance (NMR) (Fig. S2–S5†) and mass spectroscopy (Fig. S6†). On the contrary, the conformational isomers of PFODPA and its precursor show no observable polarity differences and are thus unable to be separated.

### General characterization of polyimide films

The commercially available fluorine-containing dianhydride and diamine monomers 6FDA and TFMB were chosen for polymerization with PFODA and PFODPA in consideration of their efficient roles in lowering the dielectric permittivity and enhancing the optical transparency of polyimide films. One-step polycondensation at elevated temperature in the solvent *m*-cresol was carried out to obtain fluorine-containing poly-



**Scheme 1** (a) Chemical structures of polyimide monomers studied in this work and the optimized conformations of the PFODA isomers. (b) Chemical structures of the synthesized polyimides. (c) Synthesis routes for the PFCB-containing monomers.

imides (Scheme 1). As shown in Table S2,† all the 6FDA-PFODA and PFODPA-TFMB polyimides were obtained with high molecular weight, except for PFODPA-PFODA. We speculate that the irregular conformations of both PFCB-dianhydride and PFCB-diamine would hinder chain growth, resulting in a great deal of macrocycle and oligomer formation. To verify the effect of the PFCB component on polymerization, a mixture of 6FDA and PFODPA (1:1 molar ratio) was copolymerized with PFODA. The molecular weight of 6FDA-*co*-PFODPA-PFODA polyimide was higher than that of pure PFODPA-PFODA, but still much lower than that of 6FDA-PFODA. The structures of polyimides were characterized using the FT-IR and NMR spectra shown in Fig. S7 and S8.† Typical characteristic peaks of polyimides can easily be found in the FT-IR spectra; the peaks at  $1785\text{ cm}^{-1}$  and  $1726\text{ cm}^{-1}$  correspond to the symmetric and asymmetric  $\text{C}=\text{O}$  stretching vibrations, those at  $1375\text{ cm}^{-1}$  and  $722\text{ cm}^{-1}$  to the C–N stretching vibration and imide ring deformation,<sup>30</sup> and that at  $963\text{ cm}^{-1}$  to the characteristic absorption of perfluorocyclobutyl aryl ether.<sup>27,28</sup> Additionally, the characteristic peaks of amide at around  $3200\text{ cm}^{-1}$  and  $1500\text{ cm}^{-1}$  disappeared, indicating the complete imidization of the polyimides. The NMR spectra (Fig. S8†) and elemental analysis (Table S3†) further verified that the fluorine-containing polyimides had been synthesized successfully.

All these PFCB-containing polyimides present broad diffraction peaks in wide-angle X-ray diffraction (WAXD), revealing their amorphous structure caused by the rather asymmetric conformation of the PFCB groups (Fig. S9†). The *d*-spacings of the main halos, which represent the packing density among the polyimide chains,<sup>31,32</sup> decrease sequentially from PFODPA-TFMB (5.94 Å) to 6FDA-PFODA-*trans* (5.85 Å), 6FDA-PFODA-*cis* (5.84 Å), PFODPA-PFODA (5.84 Å), and further to 6FDA-PFODA (5.68 Å). The loosest packing of PFODPA-TFMB indicates that it had the most distorted chain conformation resulting from the PFCB-containing dianhydride group. 6FDA-PFODA-*trans* and 6FDA-PFODA-*cis* share similar chain packing densities, and the mixture of these isomers could facilitate the loose packing in 6FDA-PFODA.

As shown in Table S4,† the relatively loose chain packing affords these fluorine-containing polyimides excellent solubility. They can dissolve in most polar solvents, *e.g.*, *N*-methylpyrrolidone (NMP), *N,N*-dimethylacetamide (DMAc), *N,N*-dimethylformamide (DMF), dimethyl sulfoxide (DMSO), *m*-cresol, acetone, tetrahydrofuran (THF), dichloromethane (DCM) and trichloromethane.

### Thermal and mechanical properties

Differential scanning calorimetry (DSC), dynamic mechanical analysis (DMA) and thermomechanical analysis (TMA) were carried out to estimate the thermal properties of these fluorine-containing polyimides.<sup>33</sup> The glass transition temperature ( $T_g$ ) values obtained using the three different approaches were compared (Fig. 1 and Table 1). 6FDA-PFODA and the polymers of its isomers show similar transition temperatures of around 250 °C *via* DSC. Specifically, the  $T_g$  value of 6FDA-PFODA-*trans*

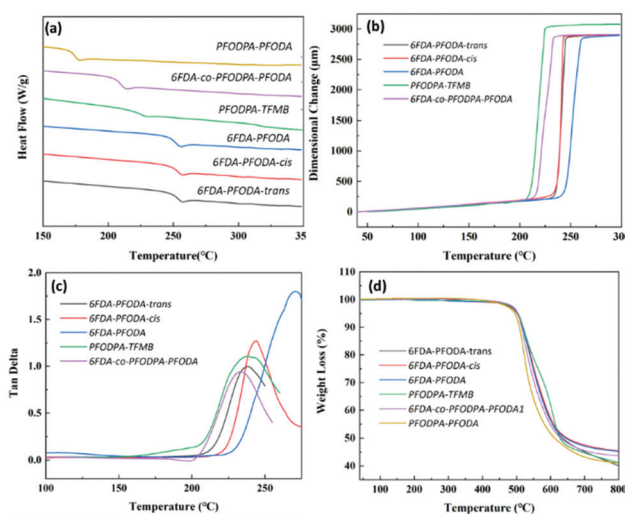


Fig. 1 Thermal properties of polyimides: (a) DSC curves of the polyimides (exo up); (b) TMA curves of the polyimides; (c)  $\tan \delta$  curves obtained from DMA; (d) TGA curves of the polyimides.

(251.5 °C) is slightly higher than of 6FDA-PFODA-*cis* (248.9 °C) due to the stiffer chain structure of the *trans* conformation.<sup>34</sup> The trends in the  $T_g$  values measured using DMA and TMA are the same as that observed in the DSC measurements. Specifically, 6FDA-PFODA shows much higher  $T_g$  values in TMA and DMA than the polymers of its isomers. On the other hand, the polyimides containing the PFCB dianhydride moiety all exhibit lower  $T_g$  values in various characterization approaches, and the transition temperature decreases with increasing PFCB content. Note that the lower  $T_g$  values of PFODPA-PFODA and 6FDA-*co*-PFODPA-PFODA could also be attributed to their relatively lower molecular weights. As revealed by WAXD, the PFCB containing dianhydride could result in looser chain packing and thus a larger free volume in the polyimides. The coefficients of thermal expansion (CTE) along the *X*–*Y* direction were also recorded using TMA. The fluorine-containing polyimides exhibit relatively high CTE values ranging from 58.7 to 70.1 ppm  $\text{K}^{-1}$  due to the loose chain packing resulting from the PFCB groups. This might be a disadvantage for their applications as high-frequency substrate materials.

The C–F bond is one of the strongest chemical bonds (484.9 kJ mol<sup>-1</sup>) in organic chemistry,<sup>35</sup> which endows the fluorine-containing polyimide films with excellent thermal stability (Fig. 1d). These polyimides exhibit similar initial decomposition temperatures of around 450 °C, which is attributed to the decomposition of the PFCB group.<sup>26–28</sup> The 5% weight loss temperatures of these films exceed 500 °C (Fig. 1d and Table 1), which is comparable to most aromatic polyimides.<sup>36,37</sup>

These polyimide films show high tensile strength values of 83.6–96.2 MPa, tensile modulus values of 2.2–3.1 GPa, and elongation at break values of 5.1–6.9% (Table 1). The 6FDA-*co*-PFODPA-PFODA film has the weakest mechanical properties,

**Table 1** Thermal and mechanical properties of polyimides

Polyimides	$T_g^a$ (°C)	$T_g^b$ (°C)	$T_g^c$ (°C)	$T_5^d$ (°C)	$T_{10}^d$ (°C)	$R_w^e$ (%)	CTE <sup>f</sup> (ppm K <sup>-1</sup> )	$\sigma_{max}^g$ (MPa)	$E^h$ (GPa)	$\epsilon^i$ (%)
6FDA-PFODA- <i>trans</i>	251.5	237.4	238.2	501.1	518.4	40.1	63.9	87.4	2.5	5.9
6FDA-PFODA- <i>cis</i>	248.9	238.1	243.7	504.1	519.4	45.4	63.5	96.2	3.1	5.8
6FDA-PFODA	250.1	247.6	261.2	503.9	518.0	45.3	58.7	88.3	2.7	5.1
PFODPA-TFMB	223.3	217.3	234.5	503.4	519.6	41.2	64.1	83.6	2.2	6.9
6FDA- <i>co</i> -PFODPA-PFODA	208.4	220.4	233.9	502.2	515.2	43.7	70.1	73.2	2.5	4.5
PFODPA-PFODA	174.4	—	—	494.9	508.6	41.1	—	—	—	—

<sup>a</sup>  $T_g$  measured using DSC at a heating rate of 10 °C min<sup>-1</sup>. <sup>b</sup>  $T_g$  recorded using TMA at a heating rate of 5 °C min<sup>-1</sup>. <sup>c</sup>  $T_g$  measured using DMA at a heating rate of 5 °C min<sup>-1</sup> at 1 Hz. <sup>d</sup> Temperatures of 5 wt% and 10 wt% weight loss. <sup>e</sup> Residual weight retention at 800 °C under a nitrogen atmosphere. <sup>f</sup> Thermal expansion coefficient recorded using TMA from 50–150 °C. <sup>g</sup> Tensile strength. <sup>h</sup> Young's modulus. <sup>i</sup> Elongation at break.

with a low tensile strength of 73.2 MPa and an elongation at break value of 3.5%. The relatively low molecular weight of the film is the main cause, due to the polymerization difficulties caused by the too-high content of PFCB groups.

### Optical properties

Fluoropolymers with good optical transparency have attracted great attention with the rapid development of the electronics industry, and are widely used in optical thin films, electronic packaging materials, large-scale integrated circuits and barrier layer coatings.<sup>38</sup> With their combination of excellent thermal and mechanical properties, fluorine-containing polyimides expand the application scenarios. The optical properties of these polyimide films measured using a UV-vis spectrophotometer are presented in Fig. 2 and Table S5.† The 6FDA-TFMB film was found to be one of the most excellent optically transparent materials among aromatic polyimides. The optical transparency of the PFCB-containing polyimides is comparable to that of the 6FDA-TFMB film. They exhibit an optical transmittance of around 70% at 400 nm and 90% at 550 nm. The cut-off wavelength ( $\lambda_0$ ) ranges from 311 nm to 335 nm. The colour intensities of the PFCB-containing polyimides are also listed in Table S5.† All the films show high  $L^*$ , negative  $a^*$ , low  $b^*$  and low haze values, indicating outstanding optical performance. The strongly distorted chain conformation and the electron-withdrawing effect of the PFCB groups play the critical

roles in inhibiting the charge transfer, affording excellent optical transparency in these PFCB-containing polyimides. It is worth noting that the PFODPA-TFMB films show inferior optical transparency (85.7% at 550 nm) compared to the other PFCB-containing polyimides (>88%). It can be inferred that the PFCB groups containing a diamine moiety contribute more to enhanced optical transparency than the PFCB groups containing a dianhydride moiety, since the electron-withdrawing effect of PFCB would produce a more electron-negative dianhydride moiety and strengthen its role as an “acceptor” for the charge transfer process.

### Dielectric properties

The dielectric properties of the fluorine-containing polyimides were measured using dielectric/impedance spectrometry, and the results are shown in Fig. 3. The dielectric constants  $D_k$  and dielectric loss  $D_f$  at 1 kHz and 10 GHz are listed in Table 2.

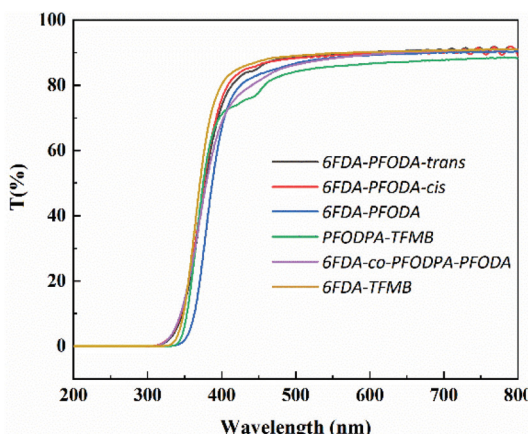


Fig. 2 Transmittance curves of various polyimide films.

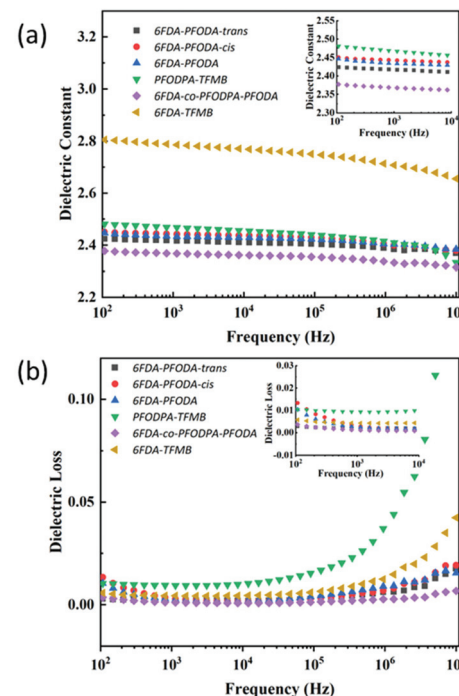


Fig. 3 (a) Dielectric constants of the polyimide films at low frequency. (b) Dielectric loss of the polyimide films at low frequency.

**Table 2** Dielectric properties and water absorption of various polyimides

	6FDA-PFODA- <i>trans</i>	6FDA-PFODA- <i>cis</i>	6FDA-PFODA	PFODPA-TFMB	6FDA- <i>co</i> -PFODPA-PFODA	6FDA-TFMB
$D_k$ at 1 kHz	2.42	2.44	2.43	2.46	2.37	2.78
$D_f$ at 1 kHz	0.0020	0.0035	0.0029	0.0094	0.0013	0.0044
$D_k$ at 10 GHz	2.59	2.62	2.60	2.53	2.50	2.91
$D_f$ at 10 GHz	0.0067	0.0049	0.0053	0.0071	0.0035	0.0048
$W_A$ (%)	0.18	0.16	0.12	0.21	0.10	0.23

These films exhibit outstanding dielectric properties with ultra-low dielectric constants (<2.5) and dielectric loss (within 0.01) at 1 kHz, which are superior to those of 6FDA-TFMB film. The underlying mechanism of their low dielectric properties can be illustrated using the Clausius–Mossotti equation:<sup>39–41</sup>

$$\frac{\epsilon - 1}{\epsilon + 2} = \frac{4\pi}{3} N \left( \alpha_e + \alpha_a + \alpha_\mu + \frac{\mu^2}{3k_b T} \right)$$

where  $\epsilon$  is the dielectric permittivity of a material;  $N$  is the dipole density;  $k_b$  is the Boltzmann constant;  $T$  is the temperature (K);  $\alpha_e$ ,  $\alpha_a$  and  $\alpha_\mu$  are the polarization of the electron, atom and induced dipole; and  $\mu$  is the dipole moment related to the orientation polarization. Below the  $T_g$ ,  $\alpha_\mu$  is tiny because of the freezing of the polymer chains. The orientation polarization of the dipole is important to the dielectric response at 10<sup>2</sup>–10<sup>7</sup> Hz, while at high frequency (10 GHz) the electron polarization ( $\alpha_e$ ) and atomic polarization ( $\alpha_a$ ) play the main roles.

As the *cis/trans*-isomers were successfully separated and the corresponding polyimide films were prepared, the conformation effect on the dielectric performance can be compared quantitatively. The optimized geometries of the 6FDA-PFODA-*trans* and 6FDA-PFODA-*cis* units are shown in Fig. S10.† The dihedral angle between the phenyl and imide rings changes slightly ( $\varphi_2 = 40.2^\circ$ ) compared with that of 6FDA-TFMB ( $\varphi_2 = 38.3^\circ$ ). The dipole moment ( $\mu$ ) and polarizability ( $\alpha$ ) of each unit were calculated *via* the DFT (CAM-B3LYP/6-311++G(d,p)) method that we previously used<sup>42</sup> and are summarized in Table 3. The introduction of PFCB groups breaks the electronic conjugation of the diamine and increases the length of the repeat unit, resulting in a low dipole moment. A lower dipole moment was achieved in all the PFCB-containing polyimides compared with that of 6FDA-TFMB. Because of the more symmetric conformation, a much lower  $\mu$  (2.21 Debye) is obtained for 6FDA-PFODA-*trans* than for 6FDA-PFODA-*cis* (3.71 Debye).

The polarizability ( $\alpha$ ) increases to 450 a.u. for 6FDA-PFODA-*cis/trans*.

Additionally, the polyimide chain packings as quantified by the packing coefficients ( $K_p$ ) were explored to evaluate the density of dipoles.<sup>43</sup> Low  $K_p$  values correspond to loose PI chain packing with a large free volume. The incorporation of PFCB groups decreases the  $K_p$  values of 6FDA-PFODA-*cis/trans*. Hence, 6FDA-PFODA-*cis/trans* with relatively loose chain packing exhibit low dielectric permittivity ( $D_{k,10\text{ GHz}} = 2.59$  and 2.62, respectively). 6FDA-PFODA-*trans* has a higher  $K_p$  value (0.708) than 6FDA-PFODA-*cis* (0.695) due to its more symmetric nature. Nevertheless, a higher dielectric permittivity value was obtained in 6FDA-PFODA-*cis*, which was mainly attributed to its large polarizability per unit volume ( $\alpha/V_{\text{vdw}} = 1.030$ ).<sup>40,44</sup> The rigid 6FDA-TFMB was found to have highly dense chain packing using WAXD (Fig. S9†) and exhibits the largest  $K_p$  (0.723), affording the largest dielectric permittivity ( $D_{k,10\text{ GHz}} = 2.91$ ).

Furthermore, an even lower dielectric permittivity ( $D_{k,10\text{ GHz}} = 2.53$ ) was found for PFODPA-TFMB, as well as for the multicomponent co-PI 6FDA-*co*-PFODPA-PFODA sample constructed from the dianhydride-containing PFCB monomer. Apparently, PFODPA-TFMB with either the *trans* or *cis* conformation exhibits a lower chain packing density, as validated by both the WAXD (Fig. S9†) and packing coefficient calculation (Table 3). The best dielectric performance was realized in the multicomponent 6FDA-*co*-PFODPA-PFODA, *i.e.*,  $D_{k,1\text{ kHz}} = 2.37$ ,  $D_{f,1\text{ kHz}} = 0.0013$ ,  $D_{k,10\text{ GHz}} = 2.5$ , and  $D_{f,10\text{ GHz}} = 0.0035$ . This could be rationalized by the fact that 6FDA-*co*-PFODPA-PFODA has the highest content of PFCB groups among all the tested samples in Table 2. These PFCB groups would result in lower  $\alpha/V_{\text{vdw}}$  and  $K_p$  values to decrease  $D_k$ , as well as a lower dipole moment density to reduce the dielectric loss. Currently, there are few well-established theories to explain the dielectric loss. In general, these PFCB-containing polyimides have relatively low dielectric loss values comparable to that of 6FDA-TFMB.

**Table 3** Molecular parameter calculations relevant to the dielectric permittivity of polyimides

Polyimide	$\rho$ (g cm <sup>-3</sup> )	$M$ (g mol <sup>-1</sup> )	$\mu$ (Debye)	$\alpha$ (a.u.)	$V_{\text{vdw}}$ (cm <sup>3</sup> mol <sup>-1</sup> )	$\alpha/V_{\text{vdw}}$	$K_p$
6FDA-PFODA- <i>trans</i>	1.246	786.5	2.21	452.16	446.66	1.012	0.708
6FDA-PFODA- <i>cis</i>	1.249	786.5	3.71	450.66	437.43	1.030	0.695
PFODPA- <i>trans</i> -TFMB	1.241 <sup>a</sup>	772.5	2.46	443.47	439.66	1.009	0.706
PFODPA- <i>cis</i> -TFMB	1.241 <sup>a</sup>	772.5	3.91	439.57	427.95	1.027	0.688
6FDA-TFMB	1.283	728.5	4.55	416.79	410.54	1.015	0.723

$\rho$ : experimental density;  $M$ : molecular weight of repeat unit;  $\mu$ : dipole moment;  $\alpha$ : polarizability;  $V_{\text{vdw}}$ : van der Waals volume;  $K_p$ : packing coefficient of the polyimides.  $\mu$ ,  $\alpha$ ,  $V_{\text{vdw}}$  were calculated using DFT (CAM-B3LYP/6-311++G(d,p)), a.u. for  $\alpha$  is Bohr<sup>3</sup> per atom and 1 Bohr = 0.52917 Å.

<sup>a</sup>The density value was measured from the isomer mixtures in PFODPA-TFMB.

Moisture can significantly impact the dielectric constant due to the large polarity of water molecule, which is a key issue in application. The water absorption of the materials was measured after immersion in deionized water for 72 h at room temperature (Table 2). The PFCB-containing polyimides have extremely low water absorption values ranging from 0.1–0.21%. The contact angles of the PFCB-containing polyimides were also found to all be above 90° (Fig. S11†). These results indicate that the polyimides are rather hydrophobic, and the values of the water contact angles were consistent with the trends in the water absorption experiments.

## Conclusions

In summary, a series of perfluorocyclobutyl aryl ether-containing polyimides were designed and synthesized. All the PFCB-containing polyimides present looser chain packings and lower glass transition temperatures than the classical transparent polyimide 6FDA-PFMB. The strongly distorted chain conformation combined with the electron-withdrawing effect of the PFCB groups endows these PFCB-containing polyimides with excellent optical transparency. As expected, these films exhibited outstanding dielectric properties with ultra-low dielectric constant and dielectric loss values at 1 kHz and 10 GHz, which were superior to those of a 6FDA-TFMB film. The copolymerized 6FDA-*co*-PFODPA-PFODA even has dielectric permittivity and dielectric loss values as low as 2.50 and 0.0035 at high frequency (10 GHz), thanks to its loose chain packing and low polarizability. In particular, we studied the conformation effect on the properties of the polyimides constructed from the PFODA diamine monomers. The differences between the glass transition temperatures and optical transparencies of 6FDA-PFODA-*trans* and 6FDA-PFODA-*cis* were small, while the 6FDA-PFODA-*trans* film exhibited slightly lower dielectric permittivity. Although the thermal stability was partially sacrificed, the good mechanical properties, high optical transparency, and rather low dielectric permittivity and dielectric loss, as well as the low water absorption, of these PFCB-containing polyimides make them attractive in potential applications in the microelectronics industry.

## Conflicts of interest

There are no conflicts to declare.

## Acknowledgements

This work was financially supported by the Key-Area Research and Development Program of Guangdong Province (No. 2020B010182002), Natural Science Foundation of Guangdong Province (No. 2022A1515010125), the Recruitment Program of Guangdong (No. 2016ZT06C322), and the Major Program of National Natural Science Foundation of China (No. 51890871).

## Notes and references

- 1 M. Li, J. Sun and Q. Fang, *Polym. Chem.*, 2021, **12**, 4501–4507.
- 2 T. Cheng, G. Lv, Y. Li, H. Yun, L. Zhang, Y. Deng, L. Lin, X. Luo and J. Nan, *Macromol. Mater. Eng.*, 2021, **306**, 2100086.
- 3 D. L. Zhou, J. H. Li, Q. Y. Guo, X. Lin, Q. Zhang, F. Chen, D. Han and Q. Fu, *Adv. Funct. Mater.*, 2021, **31**, 2102074.
- 4 Y. Zhang, Z. Liu, X. Zhang and S. Guo, *Ind. Eng. Chem. Res.*, 2021, **60**, 11749–11759.
- 5 R. Bei, C. Qian, Y. Zhang, Z. Chi, S. Liu, X. Chen, J. Xu and M. P. Aldred, *J. Mater. Chem. C*, 2017, **5**, 12807–12815.
- 6 A. M. Evans, A. Giri, V. K. Sangwan, S. Xun, M. Bartnoff, C. G. Torres-Castañedo, H. B. Balch, M. S. Rahn, N. P. Bradshaw, E. Vitaku, D. W. Burke, H. Li, M. J. Bedzyk, F. Wang, J. L. Bredas, J. A. Malen, A. J. H. McGaughey, M. C. Hersam, W. R. Dichtel and P. E. Hopkins, *Nat. Mater.*, 2021, **20**, 1142–1148.
- 7 G. Maier, *Prog. Polym. Sci.*, 2001, **26**, 3–65.
- 8 M. Xie, M. Li, Q. Sun, W. Fan, S. Xia and W. Fu, *Mater. Sci. Semicond. Process.*, 2022, **139**, 106320.
- 9 L. Fang, J. Zhou, C. He, Y. Tao, C. Wang, M. Dai, H. Wang, J. Sun and Q. Fang, *Polym. Chem.*, 2020, **11**, 2674–2680.
- 10 L. Si, D. Guo, G. Xie and J. Luo, *ACS Appl. Mater. Interfaces*, 2014, **6**, 13850–13858.
- 11 F. Hu, L. An, A. T. Chivate, Z. Guo, S. V. Khuje, Y. Huang, Y. Hu, J. Armstrong, C. Zhou and S. Ren, *Chem. Commun.*, 2020, **56**, 2332–2335.
- 12 D. Ji, T. Li, W. Hu and H. Fuchs, *Adv. Mater.*, 2019, **31**, 1806070.
- 13 W. Zheng, T. Yang, L. Qu, X. Liang, C. Liu, C. Qian, T. Zhu, Z. Zhou, C. Liu, S. Liu, Z. Chi, J. Xu and Y. Zhang, *Chem. Eng. J.*, 2022, **436**, 135060.
- 14 F. Jiang, X. Wang and D. Wu, *Energy*, 2016, **98**, 225–239.
- 15 M. Li, X. Chen, X. Li, J. Dong, X. Zhao and Q. Zhang, *ACS Appl. Mater. Interfaces*, 2021, **13**, 43323–43332.
- 16 A. Alamri, C. Wu, S. Nasreen, H. Tran, O. Yassin, R. Gentile, D. Kamal, R. Ramprasad, Y. Cao and G. Sotzing, *RSC Adv.*, 2022, **12**, 9095–9100.
- 17 C. Wang, S. Cao, W. Chen, C. Xu, X. Zhao, J. Li and Q. Ren, *RSC Adv.*, 2017, **7**, 26420–26427.
- 18 C. Wang, X. Zhao, G. Li and J. Jiang, *Polym. Degrad. Stab.*, 2009, **94**, 1526–1532.
- 19 C. Qian, R. Bei, T. Zhu, W. Zheng, S. Liu, Z. Chi, M. P. Aldred, X. Chen, Y. Zhang and J. Xu, *Macromolecules*, 2019, **52**, 4601–4609.
- 20 S. J. Park, H. S. Kim and F. L. Jin, *J. Colloid Interface Sci.*, 2005, **282**, 238–240.
- 21 X. Zhao, J. Liu, H. Yang, L. Fan and S. Yang, *Eur. Polym. J.*, 2008, **44**, 808–820.
- 22 S. Han, Y. Li, F. Hao, H. Zhou, S. Qi, G. Tian and D. Wu, *Eur. Polym. J.*, 2021, **143**, 110206.
- 23 J. Zhou, Y. Tao, X. Chen, X. Chen, L. Fang, Y. Wang, J. Sun and Q. Fang, *Mater. Chem. Front.*, 2019, **3**, 1280–1301.
- 24 D. W. Smith, H. W. Boone, R. Traiphop, H. Shah and D. Perahia, *Macromolecules*, 2000, **33**, 1126–1128.

25 B. Farajidizaji, E. I. Borrego, S. Athukorale, M. Jazi, B. Donnadieu, C. U. Pittman and D. W. Smith, *Macromolecules*, 2021, **54**, 7666–7672.

26 H. Liu, S. Zhang, C. Feng, Y. Li, G. Lu and X. Huang, *Polym. Chem.*, 2015, **6**, 4309–4318.

27 M. Jia, M. Zhou, Y. Li, G. Lu and X. Huang, *Polym. Chem.*, 2018, **9**, 920–930.

28 M. Jia, Y. Li, C. He and X. Huang, *ACS Appl. Mater. Interfaces*, 2016, **8**, 26352–26358.

29 B. K. Spraul, S. Suresh, J. Jin and D. W. Smith, *J. Am. Chem. Soc.*, 2006, **128**, 7055–7064.

30 J. Hu, Z. Wang, Z. Lu, C. Chen, M. Shi, J. Wang, E. Zhao, K. Zeng and G. Yang, *Polymer*, 2017, **119**, 59–65.

31 J. Wakita, S. Jin, T. J. Shin, M. Ree and S. Ando, *Macromolecules*, 2010, **43**, 1930–1941.

32 K. Takizawa, J. Wakita, M. Kakiage, H. Masunaga and S. Ando, *Macromolecules*, 2010, **43**, 2115–2117.

33 J. A. Hiltz and I. A. Keough, *Thermochim. Acta*, 1992, **212**, 151–162.

34 Q. Ma, X. Leng, L. Han, P. Liu, C. Li, S. Zhang, L. Lei, H. Ma and Y. Li, *Polym. Chem.*, 2020, **11**, 2708–2714.

35 G. Yan, K. Qiu and M. Guo, *Org. Chem. Front.*, 2021, **8**, 3915–3942.

36 Q. Wu, X. Ma, F. Zheng, X. Lu and Q. Lu, *Eur. Polym. J.*, 2019, **120**, 109235.

37 I. C. Tang, M. W. Wang, C. H. Wu, S. A. Dai, R. J. Jeng and C. H. Lin, *RSC Adv.*, 2017, **7**, 1101–1109.

38 J. Lv and Y. Cheng, *Chem. Soc. Rev.*, 2021, **50**, 5435–5467.

39 Z. M. Dang, J. K. Yuan, J.-W. Zha, T. Zhou, S.-T. Li and G.-H. Hu, *Prog. Mater. Sci.*, 2012, **57**, 660–723.

40 X. Li, H. Lei, J. Guo, J. Wang, S. Qi, G. Tian and D. Wu, *J. Appl. Polym. Sci.*, 2019, **136**, 47989.

41 T. Zhu, Q. Yu, W. Zheng, R. Bei, W. Wang, M. Wu, S. Liu, Z. Chi, Y. Zhang and J. Xu, *Polym. Chem.*, 2021, **12**, 2481–2489.

42 H. Lei, X. Li, J. Wang, Y. Song, G. Tian, M. Huang and D. Wu, *Chem. Phys. Lett.*, 2022, **786**, 139131.

43 E. Fujiwara, H. Fukudome, K. Takizawa, R. Ishige and S. Ando, *J. Phys. Chem. B*, 2018, **122**, 8985–8997.

44 C.-C. Kuo, Y.-C. Lin, Y.-C. Chen, P.-H. Wu, S. Ando, M. Ueda and W.-C. Chen, *ACS Appl. Polym. Mater.*, 2020, **3**, 362–371.